

Nuclear Data Evaluations of Neutron and Proton Incidence on Zr, Nb, and W for Energy up to 200 MeV

Satoshi KUNIEDA, Nobuhiro SHIGYO, Kenji ISHIBASHI

*Department of Applied Quantum Physics and Nuclear Engineering, Kyushu University
6-10-1 Hakozaki, Higashi-ku, Fukuoka 812-8581, Japan
e-mail: kuni@meteor.nucl.kyushu-u.ac.jp*

Neutron and proton nuclear data were evaluated on Zr, Nb, and W for energy up to 200 MeV. To execute optical model calculations, spherical optical potentials were developed to reproduce experimental data for many elements. The GNASH nuclear model code was used to evaluate light-particle production cross sections. For neutron emission, giant resonance correction came to be performed in the code system.

1. Introduction

High energy (up to several GeV) evaluated nuclear data are required for many elements to implement transport simulations, for such applications as the high-intensity neutron source and the accelerator-driven transmutation system of nuclear wastes. Evaluations are now being performed by JNDC working groups, and evaluated data files will be released as JENDL High Energy File.

Zirconium is important element because it has been applied in field of the nuclear technology, and its data are not included in LA150 evaluated data library [1]. Niobium is also important element because it has the merit as the superconductor component that will be used in the accelerator systems. And for the sake of the design of the spallation neutron source, tungsten is one of the quiet important elements as the target material. Nb, and W are included in LA150. To evaluate nuclear reaction data on these elements is relevant to the recent and future nuclear technologies.

It is efficient to evaluate nuclear reaction data by use of the Quantum Molecular Dynamics (QMD) [2] for energy up to several GeV, but QMD can not reproduce experimental data in intermediate energy region where the pre-equilibrium effect appear eminently. On the contrary, the GNASH nuclear model code [3] is based on Hauser-Feshbach statistical model for particle evaporations, and the exciton model for pre-equilibrium emissions, and it reproduce experimental data well in intermediate energy region.

For the aforementioned reasons, neutron and proton nuclear reaction data were evaluated on Zr, Nb, and W for energy up to 200 MeV. To begin with, optical model potential parameters were developed based on experimental data for medium and heavy nuclei as phenomenological approach. And light-particle production cross sections were evaluated by the GNASH code with transmission coefficients derived from the optical model analysis. All low-lying inelastic direct reaction cross sections were evaluated by Distorted Wave Born Approximation (DWBA). In addition to these model calculations, the correction of neutron scattered via excitations of giant resonance are also made with the Energy-Weighted Sum Rule (EWSR) [4] and DWBA in this work.

2. Optical model analysis

The optical model is very efficient method not only for cross section evaluations that include elastic angular distributions and total or non-elastic components, but also for derivations of transmission coefficients required in Hauser-Feshbach statistical model calculations for particle evaporations from compound nuclei. In the model, optical potential is

important parameter that must be adjusted to give good reproductions of experimental data. Problems are that the potential parameter must have energy and atomic mass number dependence, because there are not enough experimental data but for neutron total cross sections, on Zr, Nb and W, in wide energy range (above ~20 MeV). There are some global potentials, for example, neutron and proton potentials by Becchetti and Greenlees [5], neutron potential by Walter and Guss [6], nucleon potential by Young and Madland [7]. But their energy regions are limited, and accuracies on each nucleus are insufficient for use in nuclear data evaluations.

Spherical neutron optical potential was developed based on Fe, Ni, Cu, Y, Zr, Nb, Sn, W, and Pb experimental data [8] or data from systematics with the TOTELA [9] for energy up to 200 MeV. To obtain their energy dependences, parameters were searched by eye guidance with the ECIS-96 [10] calculations and graphical tool. Neutron potential parameter set obtained in this analysis is shown in table 1. Symbols of potential depths in the table are of the standard form, and E , A , and η mean the incident neutron energy, the atomic mass number and the nuclear symmetry $(N-Z)/A$. For the depth of the imaginary surface term, Woods-Saxon function form was used to describe the smooth decrease, and also to be included the mass number dependence in half decrease energy point E' to describe the neutron penetration at about nuclear surface into different nuclei.

For neutron evaluations, potential parameters were slightly modified to reproduce experimental data, especially for neutron total cross sections exactly. For proton evaluations, neutron potential parameters that were added Coulomb term and changed the sign of symmetric term were also used with slight modification to reproduce experimental data.

Neutron total cross sections for ^{90}Zr are shown in Fig 1. Evaluated values (solid line) reproduce experimental data [11][12] exactly. Proton non-elastic cross sections for W are shown in Fig 2. Because there aren't experimental data except one at about 100 MeV [13] for W, ^{181}Ta experimental data [13][14] and data from systematics were used in the evaluation. Present evaluation is compared with calculations used global potentials in the figure, and the comparison with LA150 was also performed. The evaluation was based on data from systematics rather than Kirkby's data above ~80 MeV. Neutron and proton elastic angular distribution cross sections are shown in Fig 3 and Fig 4 with experimental data [15-24] for ^{90}Zr . Evaluated values reproduce experimental data successfully in the wide energy range for neutron incidence. For proton incidence, the reproductions are reasonably well though over estimations for back angles are seen in some energy points.

3. Particle production cross sections

To evaluate light-particle production cross sections, the GNASH nuclear model code was used for energy up to 200 MeV. Transmission coefficients required in the Hauser-Feshbach statistical model were derived from the optical model. Neutron and proton potentials described above section are used in incident and outgoing channels. In outgoing channels of composite particles, Lohr and Haeberli's potential [25] was used for deuteron, Becchetti and Greenlees's for triton and helium-3, Avrigeanu's [26] was used for alpha particle. Ignatyuk's parameter [27] was used in Fermi gas level density. Low-lying in-elastic direct reaction cross sections were obtained by DWBA with the DUWCK-4 code. Deformation parameters for each nuclear level were taken from Reference Input Parameter Library (RIPL) [28].

An example angle-integrated cross section is shown in Fig 5 for $^{90}\text{Zr}(p, xn)$. The evaluated values reproduce experimental data at 90 MeV [29] well. For double differential cross section evaluations, the Kalbach's systematics [30] was used with result of the GNASH calculations. Examples of double differential cross section are shown in Fig 6 for (p, xn) on

^{90}Zr at 90 MeV, and Fig 7 for (p, xp) on ^{93}Nb at 65 MeV. Evaluated values reproduce 90 MeV experimental data [29] and 65 MeV experimental data [31] on each element reasonably well.

In Addition to these model calculations, corrections of neutron emission via excitations of the giant resonance (GR) were performed with Lorentzian shaped function, as follow equation [32].

$$\left(\frac{d\sigma}{dE}\right)_{GR} = \sum_l \sigma_l^{DWBA} \frac{\Gamma^2}{\pi \{(E - \hbar\omega_l)^2 + \Gamma^2 / 4\}}$$

Where, E is outgoing neutron energy, and $(d/dE)_{GR}$ means the angle-integrated cross section for GR contribution. Γ is the width of resonances, and was adopted about 5 MeV. $\hbar\omega_l$ are the adjustable parameters which means the average excitation energies of GR state having multipolarity l . σ_l^{DWBA} are neutron emission cross sections via excitation of GR, and were calculated by DWBA with deformation parameters derived from Energy-Weighted Sum Rule (EWSR). Giant dipole, quadrupole and low-energy octupole resonances (GDR, GQR, and LEOR) were taken into account as well as Reference 32.

In the GNASH code, final neutron angle-integrated spectra were calculated to sum compound (CN), pre-equilibrium (PE), in-elastic (IE) and giant resonance (GR) contributions as follow equations.

$$\frac{d\sigma}{dE} = F \left(\frac{d\sigma}{dE}\right)_{CN} + \sum_i \left(\frac{d\sigma}{dE}\right)^i \quad F = 1 - \frac{1}{\sigma_{CN}} \sum_i \left[\int dE \left(\frac{d\sigma}{dE}\right)^i \right]$$

i denotes CN, PE, IE and GR. F is the reduction factor for CN contribution to preserve reaction cross sections. GR contribution was added in this work. Angle-integrated cross section for (n, xn) on ^{184}W is shown in Fig 8. These evaluated vales with the correction reproduce 26 MeV experimental data [33] very well. In Fig 9, results of differential cross sections were shown with experimental data [34]. The Kalbach's systematics was also used in evaluation, and it reproduces experimental data considerably.

4. Conclusion

Neutron and proton reaction data were evaluated on Zr, Nb, and W for energy up to 200MeV. For the evaluations, the optical model and the GNASH code was used. The giant resonance correction was also made for (n, xn) reaction. These data were connected with JENDL-3.3, compiled into ENDF format files for each element and incident particle, and will be released as low energy parts of JENDL High Energy File.

References

- [1] M. B. Chadwick, P. G. Young, S. Chiba, *et al* : *J. Nucl. Sci. Eng.*, **131**, 293-328 (1999).
- [2] K. Niita, S. Chiba, T. Maruyama, *et al* : *J. Phys. Rev.* **C37**, 2350 (1988).
- [3] P. G. Young, *et al* : LA-6947 (1977) ; LAUR-88-382 (1988).
- [4] G. R. Satchler : *J. Nucl. Phys.* **A195**, 1 (1972).
- [5] F. D. Becchetti Jr. and G. W. Greenlees : *J. Phys. Rev.* **182**, 1190 (1969).
- [6] R. L. WALTER and P. P. Guss : *Proc. Int. Nat. Conf. Nuclear Basis and Applied Science, Santa Fe, New Mexico*, 1985, ed. P. G. Young (Gordon and Breach, New York, 1986).
- [7] P. G. Young and D. G. Madland : IAEA, INDC(NDS)-335, 109 (1995).
- [8] OECD NEA DATA BANK (<http://www.nea.fr/html/dbdata/>).
- [9] T. Fukahori and K. Niita : "Program TOTELA Calculating Basic Cross Sections in Intermediate Energy Region by Using Systematics," INDC(NDS)-416.
- [10] J. Raynal : "Optical Model and Coupled-Channel Calculation in Nuclear Physics," International

Atomic Energy Agency report, IAEA SMR-9/8 (1970), p. 281.

- [11] R. W. Finlay, W. P. Abfalterer, G. Fink, E. Montei, T. Adami, P. W. Lisowski, G. L. Morgan, R. C. Haight : *J. Phys. Rev.* **C47**, 237 (1993).
- [12] J. M. Peterson, A. Bratenahl, J. P. Stoering : *J. Phys. Rev.* **120**, 521 (1960).
- [13] P. Kirkby, and W. T. Link : *Can. J. Phys.*, **44**, 1847 (1966).
- [14] R. Abegg, J. Birchall, N. E. Davison, M. S. De Jong, *et al.* : *J. Nucl. Phys.* **A324**, 109 (1979).
- [15] Y. Wang, J. Rapaport : *J. Nucl. Phys.*, **A517**, 301 (1990).
- [16] M. Ibaraki, M. Baba, *et al.* : *J. Nucl. Instrum. Methods.*, **A446/3**, 536 (2000).
- [17] K. Matsuda, H. Nakamura, *et al.* : *J. Phys. Soc. Jap.*, **22**, 1311 (1967).
- [18] W. Makofske, G. W. Greenlees, *et al.* : *J. Phys. Rev.* **C5**, 780 (1972).
- [19] J. B. Ball, C. B. Fulmer, R. H. Bassel : *J. Phys. Rev.* **B135**, 706 (1964).
- [20] L. N. Blumberg, E. E. Gross, A. Van Der Woude, A. Zucker, R. H. Bassel : *J. Phys. Rev.* **147**, 812 (1966).
- [21] C. B. Fulmer, J. B. Ball, A. Scott, M. L. Whiten : *J. Phys. Rev.* **181**, 1565 (1969).
- [22] H. Sakaguchi, M. Nakamura, K. Hatanaka, A. Goto, T. Noro, F. Ohtani, H. Sakamoto, H. Ogawa, S. Kobayashi : *J. Phys. Rev.* **C26**, 944 (1982).
- [23] V. Comparat, R. Frascaria, N. Marty, M. Morlet, A. Willis : *J. Nucl. Phys.* **A221**, 403 (1974).
- [24] A. Nadasen, P. Schwandt, P. P. Singh, W. W. Jacobs, A. D. Bacher, P. T. Debevec, M. D. Kaitchuck, J. T. Meek : *J. Phys. Rev.* **C23**, 1023 (1981).
- [25] J. Lohr and W. Haeberli : *J. Nucl. Phys.* **A232**, 381 (1974).
- [26] V. Avrigeanu, *et al.* : *J. Phys. Rev.* **C49**, 2136 (1994).
- [27] A. V. Ignatyuk, G. N. Smirenkin, and A. S. Tishin : *Sov. J. Nucl. Phys.*, **21**, 255 (1975).
- [28] Reference Input Parameter Library (<http://www-nds.iaea.or.at/ripl/>).
- [29] A. M. Kalend, B. D. Anderson, *et al.* : *J. Phys. Rev.* **C28**, 105 (1983).
- [30] C. Kalbach : *J. Phys. Rev.* **C37**, 2350 (1988).
- [31] H. Sakai, K. Hosono, N. Matsuoka, *et al.* : *J. Nucl. Phys.* **A344**, 41 (1980).
- [32] P. Demetriou, A. Marcinkowski, P. E. Hodgson : *J. Nucl. Phys.* **A596** (1996).
- [33] A. Marcinkowski, R. W. Finlay, *et al.* : *J. Nucl. Phys.* **A501**, 1 (1989).
- [34] A. Marcinkowski, R. W. Finlay, *et al.* : *J. Nucl. Phys.* **A402**, 220 (1983).

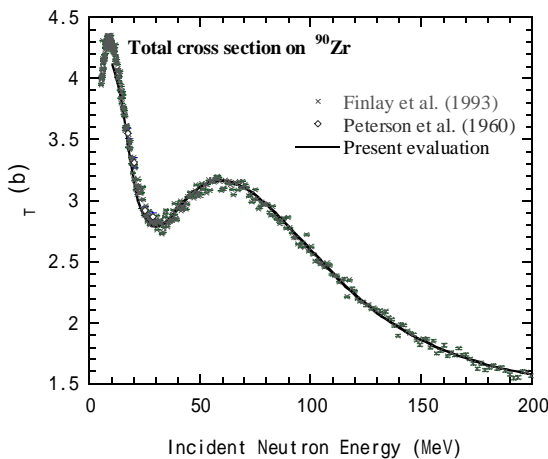


Fig 1. Neutron total cross section on ^{90}Zr .

$$V = 44.314\exp(-0.01022E) + 0.0132E - 8.9465\eta + 5.27$$

$$r_v = 1.277 - 0.000151E + 0.01E^{-1}$$

$$a_v = 0.5856 + 0.001E - 0.1E^{-1}$$

$$W = 0.005E + 14.0 / (1.0 + (130 / (E + 5.65))^{1.5})$$

$$r_w = r_v$$

$$a_w = a_v$$

$$W_d = W'_d / (1.0 + \exp((E - E') / 20.0))$$

$$W'_d = 11.398 - 7.858\eta$$

$$E' = -501.33 + 2.7059A - 48.472A^{2/3} + 291.42A^{1/3}$$

$$r_{wd} = 1.085 - 0.000139E$$

$$a_{wd} = 0.49646 + 9.3028 \times 10^{-5}A - 0.00027E$$

$$V_{so} = 6.0\exp(-0.005E)$$

$$r_{vso} = 1.017$$

$$a_{vso} = 0.6$$

$$W_{so} = 7.0 / (1.0 + \exp((E - 10.0) / 20.0))$$

$$r_{wso} = r_{vso}$$

$$a_{wso} = a_{vso}$$

(E is in MeV, and r, a are in fm)

Table 1. Neutron optical potential parameters.

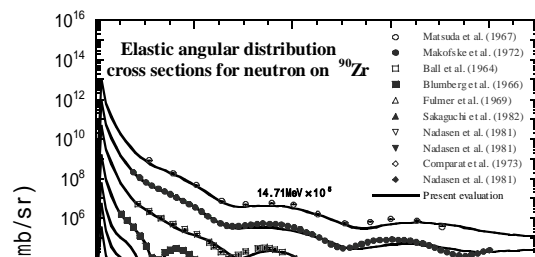
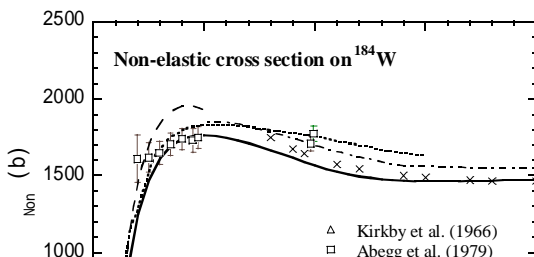


Fig 2. Proton non-elastic cross section on ^{184}W .

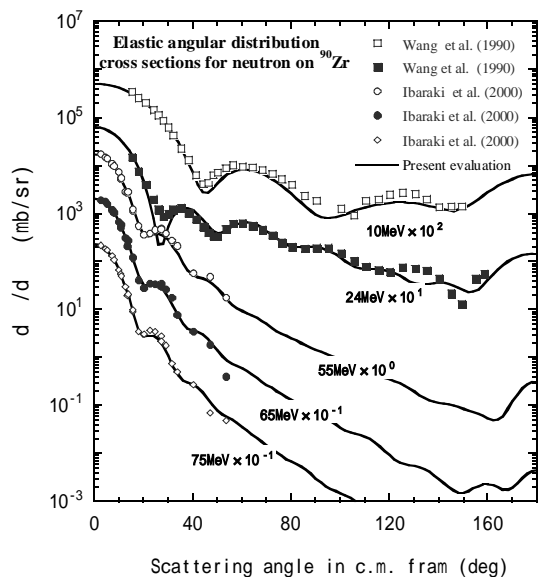


Fig 3. Neutron elastic angular distribution cross sections on ^{90}Zr .

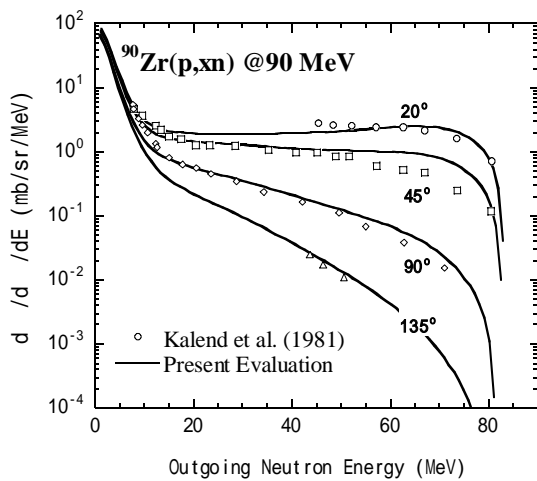


Fig 4. Proton elastic angular distribution cross sections on ^{90}Zr .

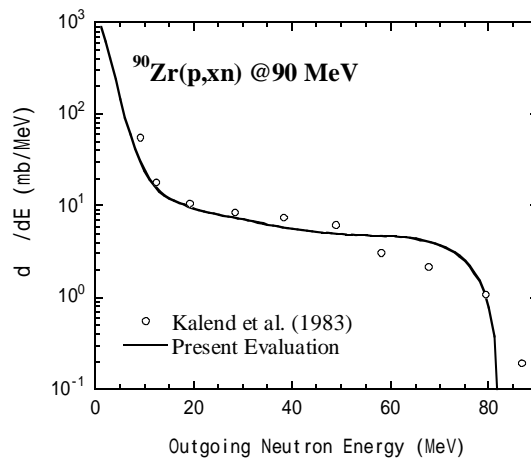


Fig 5. Angle-integrated cross section for $^{90}\text{Zr}(p,xn)$ at 90 MeV.

Fig 6. Double differential cross sections for $^{90}\text{Zr}(p,xn)$ at 90 MeV.

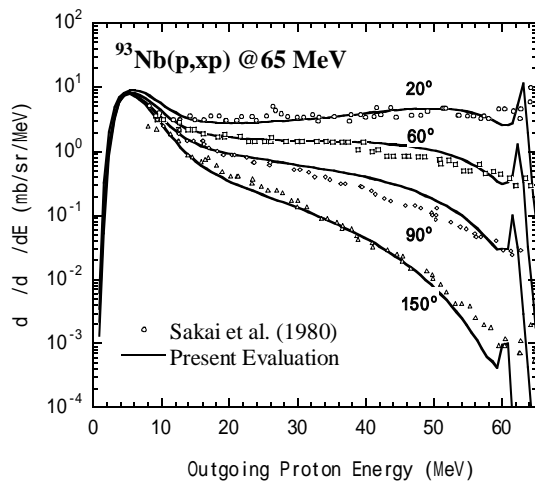


Fig 7. Double differential cross sections for $^{93}\text{Nb}(p,xp)$ at 65 MeV.

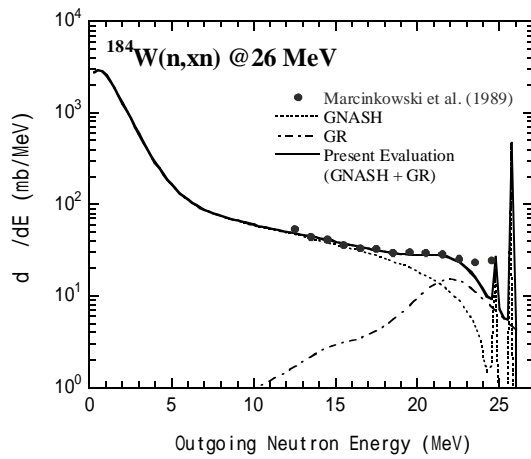


Fig 8. Angle-integrated cross section for $^{184}\text{W}(n,xn)$ at 26 MeV.

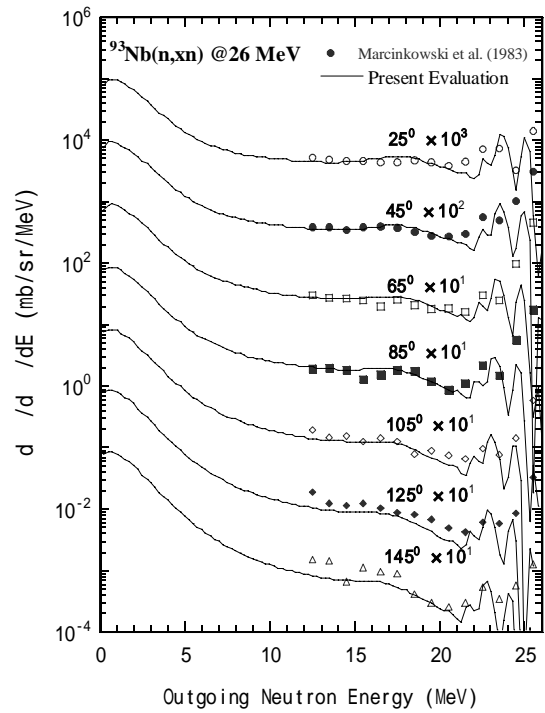


Fig 9. Double differential cross sections for $^{93}\text{Nb}(n,xn)$ at 26 MeV.